

9-1-2011

Stomatin-like protein 2 binds cardiolipin and regulates mitochondrial biogenesis and function.

Darah Christie
dchrist8@uwo.ca

Caitlin D Lemke

Isaac M Elias

Luan A Chau

Mark G Kirchhof

See next page for additional authors

Follow this and additional works at: <https://ir.lib.uwo.ca/biochempub>

 Part of the [Biochemistry Commons](#)

Citation of this paper:

Christie, Darah; Lemke, Caitlin D; Elias, Isaac M; Chau, Luan A; Kirchhof, Mark G; Li, Bo; Ball, Eric H; Dunn, Stanley D; Hatch, Grant M; and Madrenas, Joaquín, "Stomatin-like protein 2 binds cardiolipin and regulates mitochondrial biogenesis and function." (2011). *Biochemistry Publications*. 169.

<https://ir.lib.uwo.ca/biochempub/169>

Authors

Darah Christie, Caitlin D Lemke, Isaac M Elias, Luan A Chau, Mark G Kirchhof, Bo Li, Eric H Ball, Stanley D Dunn, Grant M Hatch, and Joaquín Madrenas

Stomatin-Like Protein 2 Binds Cardiolipin and Regulates Mitochondrial Biogenesis and Function

Darah A. Christie, Caitlin D. Lemke, Isaac M. Elias, Luan A. Chau, Mark G. Kirchhof, Bo Li, Eric H. Ball, Stanley D. Dunn, Grant M. Hatch and Joaquín Madrenas
Mol. Cell. Biol. 2011, 31(18):3845. DOI: 10.1128/MCB.05393-11.
Published Ahead of Print 11 July 2011.

Updated information and services can be found at:
<http://mcb.asm.org/content/31/18/3845>

	<i>These include:</i>
REFERENCES	This article cites 43 articles, 21 of which can be accessed free at: http://mcb.asm.org/content/31/18/3845#ref-list-1
CONTENT ALERTS	Receive: RSS Feeds, eTOCs, free email alerts (when new articles cite this article), more»

Information about commercial reprint orders: <http://journals.asm.org/site/misc/reprints.xhtml>
To subscribe to to another ASM Journal go to: <http://journals.asm.org/site/subscriptions/>

Stomatin-Like Protein 2 Binds Cardiolipin and Regulates Mitochondrial Biogenesis and Function[∇]

Darah A. Christie,¹ Caitlin D. Lemke,¹ Isaac M. Elias,¹ Luan A. Chau,¹ Mark G. Kirchhof,¹ Bo Li,¹ Eric H. Ball,² Stanley D. Dunn,² Grant M. Hatch,³ and Joaquín Madrenas^{1*}

The Centre for Human Immunology, Roberts Research Institute, Department of Microbiology and Immunology, and Department of Medicine,¹ and Department of Biochemistry,² The University of Western Ontario, London, Ontario, Canada N6A 5K8, and Departments of Pharmacology and Therapeutics and of Biochemistry and Medical Genetics,³ University of Manitoba, Winnipeg, Manitoba, Canada R3E 0T6³

Received 22 March 2011/Returned for modification 2 May 2011/Accepted 1 July 2011

Stomatin-like protein 2 (SLP-2) is a widely expressed mitochondrial inner membrane protein of unknown function. Here we show that human SLP-2 interacts with prohibitin-1 and -2 and binds to the mitochondrial membrane phospholipid cardiolipin. Upregulation of SLP-2 expression increases cardiolipin content and the formation of metabolically active mitochondrial membranes and induces mitochondrial biogenesis. In human T lymphocytes, these events correlate with increased complex I and II activities, increased intracellular ATP stores, and increased resistance to apoptosis through the intrinsic pathway, ultimately enhancing cellular responses. We propose that the function of SLP-2 is to recruit prohibitins to cardiolipin to form cardiolipin-enriched microdomains in which electron transport complexes are optimally assembled. Likely through the prohibitin functional interactome, SLP-2 then regulates mitochondrial biogenesis and function.

The demands for energy-generating substrates in a eukaryotic cell rise as the cell transitions from a resting state to an activated state. This process is well documented in lymphocytes undergoing mitogenic responses. In these cells, the increasing energy requirements are met by increased production of ATP either by glycolysis or by oxidative phosphorylation (OXPHOS); both processes are regulated by signaling from antigen receptors and costimulatory molecules (14–16). Scattered evidence suggests that these demands on cellular bioenergetics correlate with augmentation of the mitochondrial membrane surface and of mitochondrial numbers (8, 12, 34), a finding consistent with the key role played by these organelles in supplying most cellular ATP (14). However, the molecules that regulate mitochondrial biogenesis in response to cell activation remain mostly unknown.

Recent evidence suggests that the biogenesis of mitochondrial membranes may be regulated by the functional interactome of prohibitin 1 (PHB-1) and PHB-2 (35), but it is not known how prohibitins sense the need to increase mitochondrial membrane biogenesis. We have previously reported that SLP-2, an evolutionarily conserved mitochondrial protein belonging to the stomatin family (19, 37, 43) and enriched in detergent-insoluble microdomains of T lymphocytes, is upregulated during the activation of these cells and enhances T cell responses *in vivo* and *in vitro* (28). The function of SLP-2 is unknown. Since SLP-2 is located mostly in mitochondrial membranes and has been shown to interact with PHB-1 and PHB-2 (11), we hypothesized that upregulation of SLP-2 expression may act as a linker between PHBs and mitochondrial

biogenesis. Here we show that SLP-2 binds cardiolipin (CL) and facilitates the assembly of respiratory chain components. Upregulation of SLP-2 expression then translates into enhanced mitochondrial biogenesis and function.

MATERIALS AND METHODS

Cells. Jurkat T cells were obtained from the American Type Culture Collection (Manassas, VA). The LG2 B lymphoblastoid cell line used for antigen-presenting cells was provided by Eric Long (NIAID, NIH, Rockville, MD). Peripheral blood mononuclear cells (PBMCs) were isolated from normal donors using Ficoll-Hypaque (Amersham Pharmacia Biotech, Uppsala, Sweden). Cells were washed and resuspended at 1×10^6 /ml. PBMC blasts were generated with phorbol myristate acetate (PMA; 1 ng/ml) and ionomycin (100 ng/ml) at 37°C for 72 h.

Plasmids, small interfering RNA (siRNA), and T cell transfectants. Full-length human SLP-2 cDNA was subcloned into the pEGFPN1 expression vector (Clontech Inc., Palo Alto, CA) to create an in-frame translational fusion of SLP-2 with green fluorescent protein (GFP) at the 3' end (SLP-2-GFP) as described previously (28). The full-length SLP-2-GFP construct was placed in the doxycycline-inducible pBig2i vector (5). A doxycycline-inducible mutant of human SLP-2 lacking the amino-terminal domain tagged with GFP was also constructed. Stable transfectants were generated by nucleofection.

Upregulation of SLP-2 expression. For induction of high levels of SLP-2 expression, doxycycline (Sigma, St. Louis, MO) was added in culture at 1 μg/ml for 18 to 24 h. Parental cells, which express low levels of SLP-2, are referred to as low expressors (SLP-2^{lo}), whereas SLP-2-GFP-transfected T cells cultured in the presence of doxycycline are referred to as high expressors (SLP-2^{hi}). Transfection of pBig2iGFP, pBig2iSLP2GFP, or pmaxGFP (Amaya, Gaithersburg, MD), or mock transfection, into human PBMCs or isolated primary CD4⁺ T helper cells was conducted using the Human T Cell Nucleofector kit (Amaya). After transfection, cells were cultured for 24 h before stimulation.

Antibodies. The following monoclonal antibodies (MAb) were used in these studies: OPA-1 and DLP1 (Drp1) (BD Biosciences, Mississauga, Ontario, Canada), cytochrome *c*, complex I subunit NDUFS3, the 70-kDa subunit of complex II, complex III cor-2 subunit II of complex IV, and the alpha subunit of complex V (MitoSciences, Eugene, OR), β-actin (Santa Cruz Biotechnology, Santa Cruz, CA), and glyceraldehyde-3-phosphate dehydrogenase (GAPDH) (Chemicon International, Temecula, CA). Rabbit polyclonal antibodies against Mfn2 (Sigma, St. Louis, MO), PGC-1α (Santa Cruz Biotechnology, Santa Cruz, CA), and SLP-2 (Proteintech Group, Inc., Chicago, IL) were also used.

* Corresponding author. Present address: Duff Medical Building, Room 511, McGill University, 3775 University St., Montreal, Quebec H3A 2B4, Canada. Phone: (514) 398-3914. Fax: (514) 398-7052. E-mail: joaquin.madrenas@mcgill.ca.

[∇] Published ahead of print on 11 July 2011.

Reagents. The following working concentrations were used: 4 μM oligomycin and 1 $\mu\text{g/ml}$ ionomycin (both from Sigma). [^3H]acetate and [^{14}C]linoleic acid were obtained from Amersham (Oakville, Ontario, Canada). Lipid standards were obtained from Serdary Research Laboratories, Englewood Cliffs, NJ. Thin-layer chromatographic plates (silica gel G; thickness, 0.25 mm) were obtained from Fisher Scientific (Winnipeg, Manitoba, Canada). Ecolite scintillant was obtained from ICN Biochemicals (Montreal, Quebec, Canada). Primers for real time-PCR were obtained from Invitrogen. All other chemicals were certified ACS grade or better and were obtained from Sigma Chemical Company or Fisher Scientific.

Confocal microscopy. Confocal microscopy was performed with a Zeiss LSM 510 microscope (Carl Zeiss, Inc.) (2). Photobleaching experiments to test for mitochondrial fusion were carried out by targeting an area of MitoTracker Red CMXRos-labeled mitochondria within a cell for repeated exposure to a high-power HeNe1 laser. Loss of fluorescence at the targeted point was then compared with the fluorescence at an unrelated point within the same cell or another cell. A similar loss in fluorescent intensity from the unrelated point within the same cell indicated mitochondrial fusion between the two points.

Transmission electron microscopy. Cells were fixed in 2.5% glutaraldehyde in 0.1 M sodium cacodylate buffer for 2 h, washed in the buffer, fixed in 1% osmium tetroxide in 0.1 M sodium cacodylate buffer for 1 h, washed in the buffer again, and enrobed in Noble agar. Following a wash in distilled water, cells were stained with 2% uranyl acetate for 2 h, dehydrated through a graded series of ethanol, cleared in propylene oxide, infiltrated with Epon resin, and embedded. Thin sections were stained with 2% uranyl acetate and lead citrate and were viewed with a Philips 410 transmission electron microscope.

Measurement of mitochondrial mass. Human PBMCs were labeled with 100 nM MitoTracker Red CMXRos (Invitrogen) for 20 min at 37°C in complete RPMI 1640. Fluorescence was detected by flow cytometry and was analyzed with FlowJo flow cytometry analysis software (Tree Star, Inc., Ashland, OR). To inhibit cardiolipin synthase during *in vitro* activation, human PBMCs were stimulated with 1 ng/ml PMA and 100 ng/ml ionomycin in the presence of 4 μM triacsin C at 37°C for 24 h (22).

Measurement of cardiolipin. Human PBMCs, resting or blasted, were labeled with 10 nM nonyl acridine orange (Sigma) for 15 min at 37°C. Fluorescence was detected by flow cytometry.

Measurement of cardiolipin mass in stable SLP-2-GFP-transfected Jurkat cells. Jurkat cells stably transfected with doxycycline-inducible SLP-2-GFP were incubated without (SLP-2^{lo}) or with (SLP-2^{hi}) 1 $\mu\text{g/ml}$ doxycycline for 72 h. After incubation, the medium was aspirated, and the dishes were washed twice with 2 ml of ice-cold phosphate-buffered saline. Cells were harvested in 2 ml of methanol-water (1:1, by volume), and 25- μl aliquots were taken for protein determination (31). Subsequently, 0.5 ml of water and 2 ml chloroform were added to initiate phase separation. Samples were centrifuged at 2,000 rpm for 10 min, and the upper phase was aspirated. Two milliliters of the theoretical upper phase (methanol-0.9% NaCl-chloroform) (48:47:3, by volume) was added, and centrifugation was repeated for 5 min. The organic phase was removed, dried under nitrogen gas, and resuspended in chloroform-methanol (2:1, by volume). A 50- μl aliquot was spotted onto thin-layer plates for the separation of cardiolipin from other phospholipids as described elsewhere (35). Phospholipids were removed from the plate, and the phospholipid phosphorus content of cardiolipin was determined as described previously (39).

Radiotracer studies of *de novo* cardiolipin synthesis. SLP-2^{lo} or SLP-2^{hi} cells were grown in Dulbecco's modified Eagle medium (DMEM) with 10% fetal bovine serum (FBS), 100 U penicillin, and 100 μg streptomycin in 60-mm-diameter dishes and were incubated at 37°C under a humidified atmosphere of 5% CO₂. Cells were then incubated immediately after doxycycline treatment with 0.1 μM [^3H]acetate (10 $\mu\text{Ci/dish}$) for 16 h or with 0.1 mM [^{14}C]linoleic acid (3 $\mu\text{Ci/dish}$) bound to albumin (molar ratio, 1:1) for 8 h. Cells were harvested, and the amount of radioactivity incorporated into cardiolipin was determined as described previously (21).

Real time-PCR. The cycler protocol for real-time PCR consisted of a 30-min reverse transcription (RT) step at 50°C, followed by a 15-min *Taq* activation step at 95°C, followed by a 1-min separation at 95°C and a melting curve that increased in temperature incrementally from 60°C to 95°C over the course of 20 min. The primers used for real time-PCR were Invitrogen's D-LUX 6-carboxy-fluorescein (FAM)-labeled primer sets: for cardiolipin synthase, reverse primer CGAACCCTGGTGTGGAAGAGTT-FAM-G and forward primer CGAGA GATGTAATGTTGATTGCTG; for phosphatidylglycerol phosphate synthase, reverse primer CCGTGAGTCACTACAGGTTTGACACC-FAM-G and forward primer TCGGCCTCCAGCACATTAAG; for PGC-1 α , reverse primer TGC TTC GTC GTC AAA AAC AG and forward primer TCA GTC CTC ACT GGT GGA CA; and for 18S rRNA, reverse primer CGGGTGCTCTTAGCTGAG

TGTCC-FAM-G and forward primer CTCGGGCCTGCTTTGAACAC. Changes in mRNAs were analyzed on an Eppendorf Mastercycler ep Realplex system with software version 1.5.474, and data are presented as the mean fold change ($2^{-\Delta\Delta C_T}$) in mRNA expression relative to 18S rRNA expression (30).

Mitochondrial DNA quantification. Mitochondrial cytochrome *c* oxidase I (CCO) and the nuclear polymerase γ accessory subunit were amplified from total cellular DNA (10). Relative levels of mitochondrial DNA were determined by comparing the threshold cycle (C_T) detection values of CCO in SLP-2^{hi} and SLP-2^{lo} cells and were normalized to nuclear DNA levels by the $\Delta\Delta C_T$ method (30).

Cell lysate preparation. Cells were lysed in a 1% Triton X-100-containing buffer (1% Triton X-100, 150 mM NaCl, 10 mM Tris [pH 7.6], 5 mM EDTA, 1 mM sodium orthovanadate, 10 $\mu\text{g/ml}$ leupeptin, 10 $\mu\text{g/ml}$ aprotinin, 25 μM *p*-nitrophenyl-*p*'-guanidinobenzoate) at 4°C for 30 min. Lysates were cleared by centrifugation (10,700 $\times g$, 4°C, 10 min), mixed with sample buffer containing β -mercaptoethanol, boiled, and blotted (7).

Mitochondrion isolation. Intact mitochondria were isolated from 5×10^6 to 10×10^6 Jurkat T cells using the Qproteome Mitochondria Isolation kit (Qiagen). Mitochondrial preparations were mixed with sample buffer containing β -mercaptoethanol, boiled, and analyzed by sodium dodecyl sulfate-polyacrylamide gel electrophoresis (SDS-PAGE).

Prohibitin and SLP-2 membrane association. Mitochondria were isolated and fractionated with 0.1 M Na₂CO₃ as described previously (20). Fractions treated with H₂O were used as an input control. Soluble and membrane fractions were analyzed by immunoblotting for PHB-1 and SLP-2.

NADH dehydrogenase activity. NADH dehydrogenase activity from whole-cell lysates was measured using the complex I enzyme activity microplate assay kit (MitoSciences).

ATP quantitation. Mitochondrial and total-cell-lysate ATP levels were measured using the ATP determination kit (Molecular Probes, Eugene, OR). Briefly, 10 μl of ATP standards (ranging from 1.95 to 1,000 nM), mitochondrial fractions, or cell lysates were added in triplicate to 90 μl of a standard reaction solution in a 96-well Chromalux luminescent assay microplate (Dydx Technologies, Chantilly, VA). Sample luminescence was measured using an MLX microtiter plate luminometer (Dydx Technologies). Sample ATP concentrations were calculated from the standard curve and were normalized to cell equivalents.

T cell stimulation. Jurkat T cells were stimulated as described previously (2). A CD4⁺ T cell isolation kit and MACS (magnetic cell sorting) columns (Miltenyi Biotec, Inc., Auburn, CA) were used to isolate primary CD4⁺ T helper cells from PBMCs. pBig2iGFP-, pBig2iSLP2GFP-, pmaxGFP-, or mock-transfected PBMCs (0.2×10^6 cells/group) in the presence or absence of 1 $\mu\text{g/ml}$ doxycycline were plated in triplicate on 96-well plates with various concentrations of staphylococcal enterotoxin E (SEE) at 37°C under 5% CO₂ for 24 h. Supernatants were collected, and interleukin-2 (IL-2) was measured by an enzyme-linked immunosorbent assay (ELISA) (9).

Oxygen consumption. Cells were incubated in a 96-well oxygen biosensor system (Becton Dickinson [BD], San Jose, CA). Background fluorescence was measured before plating of cells, and specific fluorescence due to oxygen consumption was measured after 24 h of incubation at 37°C. The fluorescent signal was measured on a Safire fluorescent plate reader (Tecan, Switzerland). To calculate [O₂] from fluorescence intensity, we followed the protocol supplied by BD: [O₂] = [(DR/NRF) - 1]/K_{SV}, where NRF is normalized relative fluorescence, calculated as the fluorescence intensity of cells (*I*) divided by the fluorescence intensity of a blank well (*I*_B); DR is calculated as the fluorescence intensity of 100 mM sodium sulfite (*I*_S) divided by *I*_B; and K_{SV} is calculated as (DR - 1)/[O₂]_A, where [O₂]_A equals 195 μM at 37°C with 5% CO₂.

Induction and detection of apoptosis. T cells were treated with 5 $\mu\text{g/ml}$ of actinomycin D (Sigma) for 3 h to induce apoptosis, which was measured by flow cytometry as mitochondrial transmembrane potential ($\Delta\Psi_m$) loss using the cell-permeant probe MitoTracker Red CMXRos (Invitrogen), or as an increase in annexin V staining.

Generation of hrSLP-2. We generated a human recombinant SLP-2 (hrSLP-2) cDNA coding for amino acids 36 to 356 of human SLP-2 downstream of a sequence coding for a 6 \times His tag, a thrombin cleavage site, thioredoxin, and a tobacco etch virus (TEV) cleavage site in a pET-28 plasmid. Rosetta strain *Escherichia coli* containing plasmids was streaked, and single colonies were picked and grown to a *A*₆₀₀ of 0.5 to 0.6. The culture was cooled to 15°C and was induced with 0.1 mM isopropyl- β -D-thiogalactopyranoside (IPTG) overnight. Bacteria were pelleted, scraped into preweighed 50-ml centrifuge tubes, resuspended in 25-ml 50/10 buffer (50 mM Tris [pH 8.0], 10 mM MgCl₂), and centrifuged at 10,000 rpm for 10 min. The supernatant was decanted, and the pellet was weighed and resuspended in 10 \times (wet weight) 50/10 buffer. The buffer was fortified with 1 mM phenylmethylsulfonyl fluoride (PMSF; Sigma), 5 mM

p-aminobenzamidine (Sigma), and Complete protease inhibitor cocktail (Roche). The bacteria were lysed by two passes at 10,000 lb/in² in a French pressure cell, and the lysates were centrifuged for 10 min at 10,000 rpm at 4°C. The supernatant was decanted into 60-ml ultracentrifuge tubes, spun at 38,000 rpm at 4°C for 90 min, decanted again, and stored at -80°C.

Chromatography was run using Chelating Sepharose Fast Flow resin (GE BioScience). Two column volumes of NiSO₄ were applied to the column in order to bind the nickel. The column was equilibrated with 10 column volumes of buffer A (20 mM Tris-HCl [pH 8.0], 100 mM NaCl, 5 mM 2-mercaptoethanol, 10% glycerol, 20 mM imidazole). The sample was added to the column and was allowed to flow through the resin at a rate of approximately 0.5 ml/min. The column was washed with 10 column volumes of buffer A, followed by 2 column volumes of buffer B (20 mM Tris-HCl [pH 8.0], 1 M NaCl, 5 mM 2-mercaptoethanol, 10% glycerol) and a further 2 volumes of buffer A. Bound proteins were eluted by competitive binding with buffer C (20 mM Tris-HCl [pH 8.0], 100 mM NaCl, 5 mM 2-mercaptoethanol, 10% glycerol, 0 to 500 mM imidazole) and were collected in 1.5-ml or 5-ml fractions. Fractions were stained with Coomassie brilliant blue and were analyzed by SDS-PAGE.

Protein samples were dialyzed into 10 mM Tris (pH 8.0) overnight at 4°C. The protein solution was then brought up to 2 mM EDTA and 1 mM dithiothreitol (DTT) and was quantitated by the bicinchoninic acid (BCA) method (BCA protein assay kit; Pierce). The SLP-2 construct was then incubated with TEV protease (ratio, 1:10) at room temperature for 2 h. After cleavage, the sample was dialyzed into 10 mM Tris (pH 8.0) overnight at 4°C to remove EDTA and DTT.

Phospholipid vesicle coprecipitation assay. The phospholipid vesicle coprecipitation assay was performed as described previously (4). The required amounts of phospholipids were transferred to glass vials and were dried under a gentle stream of nitrogen gas. The required amount of binding buffer (20 mM Tris [pH 7.5], 150 mM NaCl, 1 mM EDTA) was added, and samples were incubated for 3 h at 52°C. After this incubation, hrSLP-2 protein was added to the lipid vesicle solution at a 5:1 ratio of lipid to protein and was incubated for 30 min at 37°C. Samples were centrifuged at 40,000 rpm for 10 min at room temperature; the supernatant was removed; and pellets were resuspended in binding buffer. Laemmli sample buffer was added to the supernatant and pellet fractions, boiled for 7 min, and run on an SDS-PAGE gel. Bovine heart cardiolipin was purchased from Sigma; chicken egg L- α -phosphatidylcholine (PC), L- α -phosphatidylethanolamine (PE), and L- α -phosphatidylglycerol, porcine brain L- α -phosphatidylserine, and soy L- α -phosphatidylinositol were purchased from Avanti Polar Lipids, Inc. (Alabaster, AL).

RESULTS

SLP-2 is localized mostly in mitochondria. Studies by different groups, including our own, have shown that SLP-2 in human cells is expressed in two pools (11, 20, 28). The major pool of SLP-2 is associated with the mitochondrial inner membrane, whereas a quantitatively minor pool is associated with the plasma membrane. This compartmentalization was corroborated biochemically by subcellular fractionation of human T cells (Fig. 1a). SLP-2 was detected in the membrane and organelle/cytoskeleton fractions but not in the nuclear or cytosolic compartment. Porin (voltage-dependent anion channel [VDAC]), a protein detected in mitochondrial and plasma membranes, showed a partitioning pattern similar to that of SLP-2.

To study the role of SLP-2, we developed stable transfected cells in which SLP-2 expression can be tightly regulated using a doxycycline-inducible promoter coding for a C-terminally GFP tagged SLP-2 protein (SLP-2-GFP). This system allowed us to control the levels of SLP-2 in human cells (T cells for these experiments) from very low (basal levels of expression by Jurkat T cells stably transfected with this cDNA in the absence of doxycycline; referred to below as SLP-2^{lo}) to high (10- to 100-times-higher expression upon addition of doxycycline; referred to below as SLP-2^{hi}). With these cells, we corroborated the predominant localization of SLP-2 in mitochondria both by

biochemical fractionation (Fig. 1b) and by confocal microscopy, in which SLP-2-GFP colocalized with the mitochondrial dye MitoTracker Red (Fig. 1c and d). Such an intracellular distribution was determined by an N-terminal mitochondrial targeting sequence (11, 20), as evidenced by the fact that SLP-2-GFP deletion mutants lacking the N terminus abrogated mitochondrial localization, whereas expression of the SLP-2 N-terminal domain fused to GFP was sufficient to determine mitochondrial localization of this protein (data not shown) (11).

Upregulation of SLP-2 expression increases mitochondrial biogenesis. To learn about the function of SLP-2, given its mitochondrial localization, we first examined the effect of induction of SLP-2 expression on mitochondrial mass by using the system mentioned above. We found that upregulation of SLP-2 expression, but not of a control protein, induced a significant increase in the mass of metabolically active mitochondria ($P < 0.01$), as determined with the intact mitochondrial label MitoTracker Red (Fig. 2a and b), and a significant increase in the number of mitochondria per T cell ($P < 0.001$) (Fig. 2c and d). Such mitochondrial biogenesis required appropriate targeting of SLP-2 to mitochondria, as evidenced by the fact that overexpression of a SLP-2-GFP mutant lacking the N-terminal mitochondrial targeting sequence (Δ NSLP-2) did not induce a significant increase in the number of mitochondria (Fig. 2c and d), although a slight increase over the baseline was observed, likely due to limited transport of the mutant as a dimer with endogenous full-length SLP-2. Furthermore, the increased mitochondrial mass observed after upregulation of SLP-2 expression was corroborated by flow cytometry for primary human leukocytes from peripheral blood in the transition from the resting state (in which they express low levels of SLP-2) to the primed blasted state (in which they express high levels of SLP-2) (Fig. 2e and f).

Mitochondrial biogenesis requires *de novo* synthesis of cardiolipin, a phospholipid in the mitochondrial membrane. Since upregulation of SLP-2 expression was associated with increased mitochondrial biogenesis, we next tested whether SLP-2 overexpression increased cardiolipin synthesis. A 37% increase in cardiolipin content (as a percentage of the total phospholipid phosphorus mass) was detected in SLP-2^{hi} cells (Fig. 3a). This finding was corroborated in human PBMCs transitioning from the resting state (i.e., expressing low levels of SLP-2) to the activated state (i.e., expressing high levels of SLP-2) by flow cytometry with the cardiolipin dye nonyl acridine orange (Fig. 3b). Since the loading and retention of this dye are sensitive to changes in mitochondrial potential (25), we verified that the increase in cardiolipin content was due to *de novo* synthesis of this phospholipid by using radiolabeling assays incubating SLP-2^{lo} and SLP-2^{hi} cells with [³H]acetate and [¹⁴C]linoleic acid, both of which are incorporated into newly synthesized cardiolipin. SLP-2^{hi} cells showed higher levels of radiolabeled cardiolipin under both incubation conditions than did SLP-2^{lo} cells ($P < 0.05$) (Fig. 3c and d). Finally, we used real time RT-PCR to look at the levels of phosphatidylglycerol phosphate synthase mRNA and cardiolipin synthase mRNA, since these resulting enzymes are involved in the final steps of cardiolipin biosynthesis. As expected, the SLP-2^{hi} cells had consistently higher transcript levels of both enzymes (Fig. 3e and f), consistent with a state of activation of lipid biosynthesis

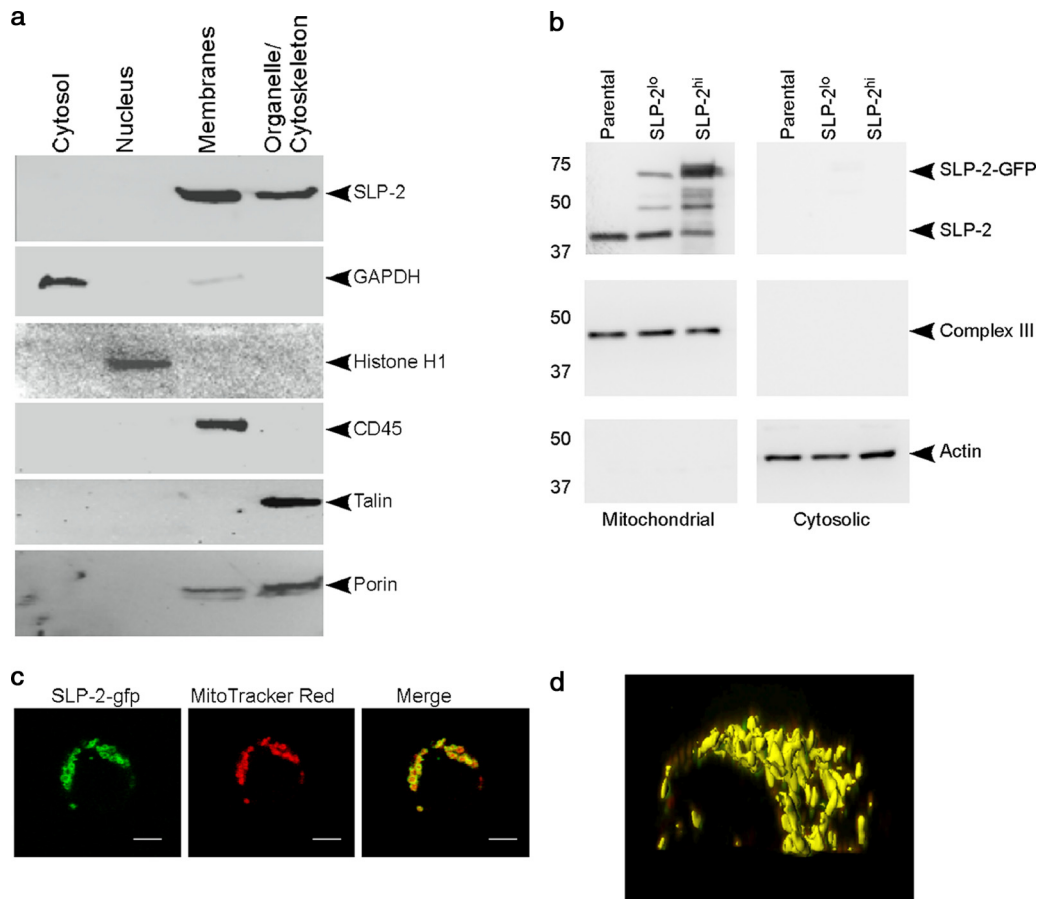


FIG. 1. The major pool of SLP-2 in human T cells is located in mitochondria. (a) Subcellular fractions of Jurkat T cells were isolated by differential centrifugation and were immunoblotted for SLP-2. Serial blotting for GAPDH, histone H1, CD45, and talin was performed to control for the quality of the fractions. Blotting of porin (VDAC), another protein with a major subcellular pool in the mitochondrial fraction and a smaller pool in the plasma membrane, is also shown. (b) Mitochondrial and cytosolic fractions of stable T cell SLP-2-GFP transfectants expressing low (SLP-2^{lo}) and high (SLP-2^{hi}) levels of SLP-2-GFP were isolated by differential centrifugation and were immunoblotted for SLP-2, electron transport complex III, and β -actin. Note that in addition to the endogenous SLP-2 and SLP-2-GFP forms, we detected bands likely reflecting intermediate SLP-2 degradation fragments. (c) Stably expressed SLP-2-GFP colocalizes with MitoTracker Red CMXRos by confocal microscopy. Bars, 5 μ m. (d) Three-dimensional reconstitution image analysis. A lateral view of a T cell attached to a glass slide is shown. The yellow units represent mitochondria and the mitochondrial network. Images are representative of more than 100 cells from more than 5 independent experiments.

at the transcriptional level. Together, these data led us to conclude that SLP-2 regulates cardiolipin synthesis, which is required for the formation of mitochondrial membranes. To examine the requirement of cardiolipin synthase upregulation for mitochondrial biogenesis in SLP-2^{hi} cells, PBMCs were activated with 1 ng/ml PMA and 100 ng/ml ionomycin in the presence of 4 μ M triacsin C, an inhibitor of cardiolipin synthase. Under these conditions, the increase in mitochondrial mass upon T cell activation was blocked (Fig. 3g), indicating a requirement for cardiolipin synthesis in mitochondrial biogenesis induced by SLP-2 upregulation.

In addition to membrane formation, mitochondrial biogenesis also requires activation of a nuclear transcription program that encodes the majority of mitochondrial proteins. This nuclear transcriptional program is dependent on PGC-1 α , a transcriptional coactivator and master regulator of mitochondrial biogenesis (40). Thus, we performed real-time RT-PCR to measure the levels of PGC-1 α mRNA and found that these

were increased in SLP-2^{hi} cells (Fig. 3h), supporting the idea that upregulation of SLP-2 expression is associated with an increase in the expression of mitochondrially targeted genes. Of interest, induction of SLP-2 expression also resulted in significant increases in the levels of OPA-1 and mitofusin-2 ($P < 0.05$), both integral mitochondrial membrane proteins associated with mitochondrial fusion, but not in the levels of Drp1 (involved in mitochondrial fission), GAPDH, or cytochrome *c* (data not shown). However, the increases in OPA-1 and mitofusin-2 levels did not translate functionally into enhanced mitochondrial fusion.

Mitochondrial biogenesis requires replication of mitochondrial DNA. As expected from the data presented above, we found that upregulation of SLP-2 correlated with a 70% increase in the level of mitochondrial DNA (Fig. 3i). Taken together, these findings lead us to conclude that higher levels of SLP-2 stimulate cardiolipin synthesis and mitochondrial biogenesis.

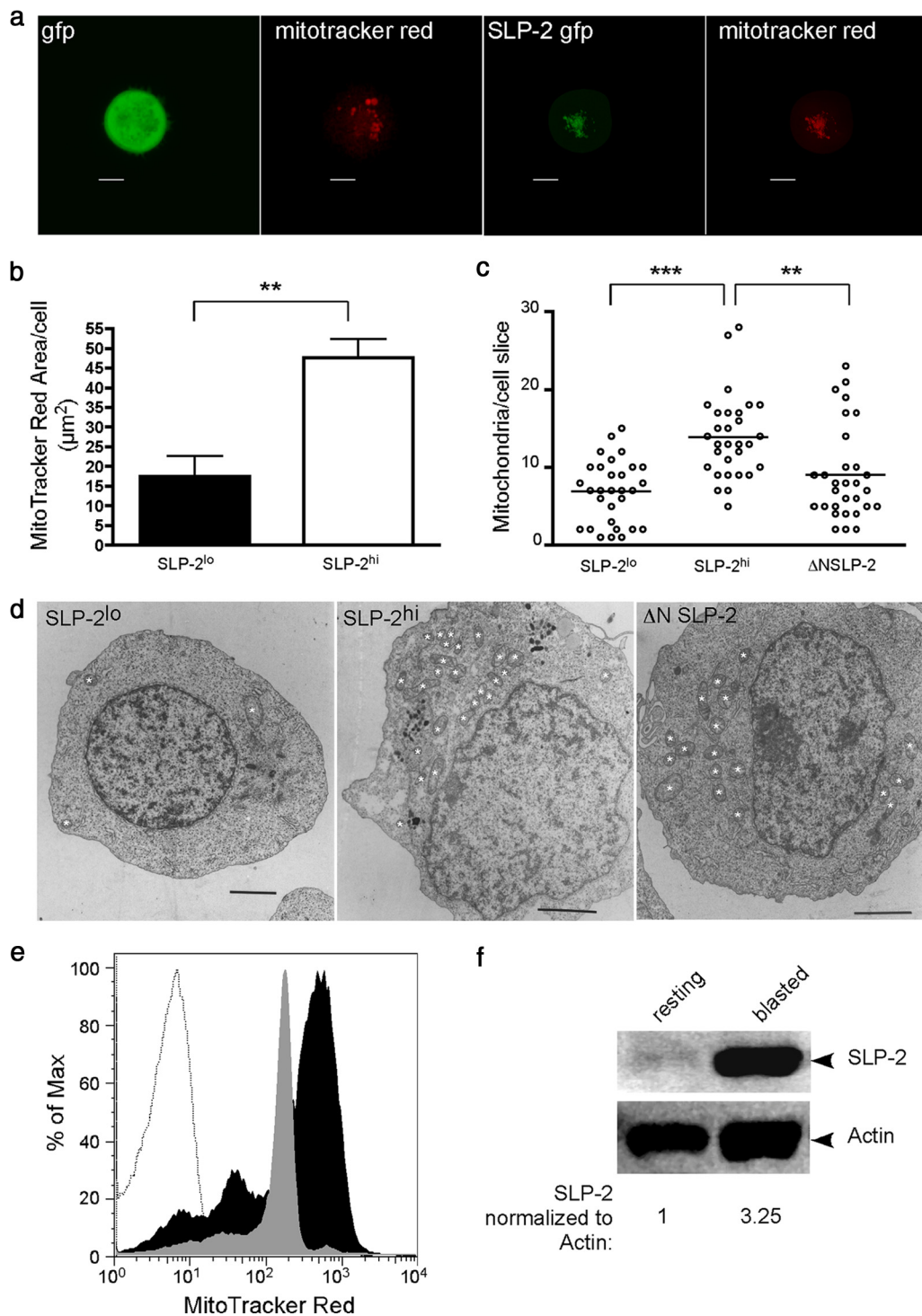


FIG. 2. Induction of SLP-2 expression triggers mitochondrial biogenesis in human T cells. (a and b) T cells expressing high levels of SLP-2 (SLP-2^{hi}) and GFP-expressing control cells, which contain lower levels of SLP-2 (SLP-2^{lo}), were stained with MitoTracker Red, and the signal was quantified in each cell. Bars, 5 μm . (c) Mitochondria visualized by transmission electron microscopy were counted for 30 cell slices of SLP-2^{hi} T cells, SLP-2^{lo} T cells, or T cells expressing a SLP-2 mutant in which the N-terminal mitochondrial targeting sequence was deleted ($\Delta\text{NSLP-2}$). Asterisks indicate significant differences (***, $P < 0.001$; **, $P < 0.01$) as determined by Student's *t* test. (d) Representative transmission electron microscopy images of SLP-2^{lo}, SLP-2^{hi}, and $\Delta\text{NSLP-2}$ T cells. Mitochondria are indicated by asterisks. Bars, 2 μm . (e) Mitochondrial mass was measured by flow cytometry in resting (gray) and activated (black) human peripheral blood mononuclear cells after labeling with MitoTracker Red. The result for the unstimulated control is shown by a dotted line. (f) Immunoblotting of PBMC whole-cell lysates for SLP-2 demonstrated that SLP-2 levels were upregulated after blasting. β -Actin blotting was used as a loading control. Densitometric units of SLP-2 for each group normalized for actin levels are shown.

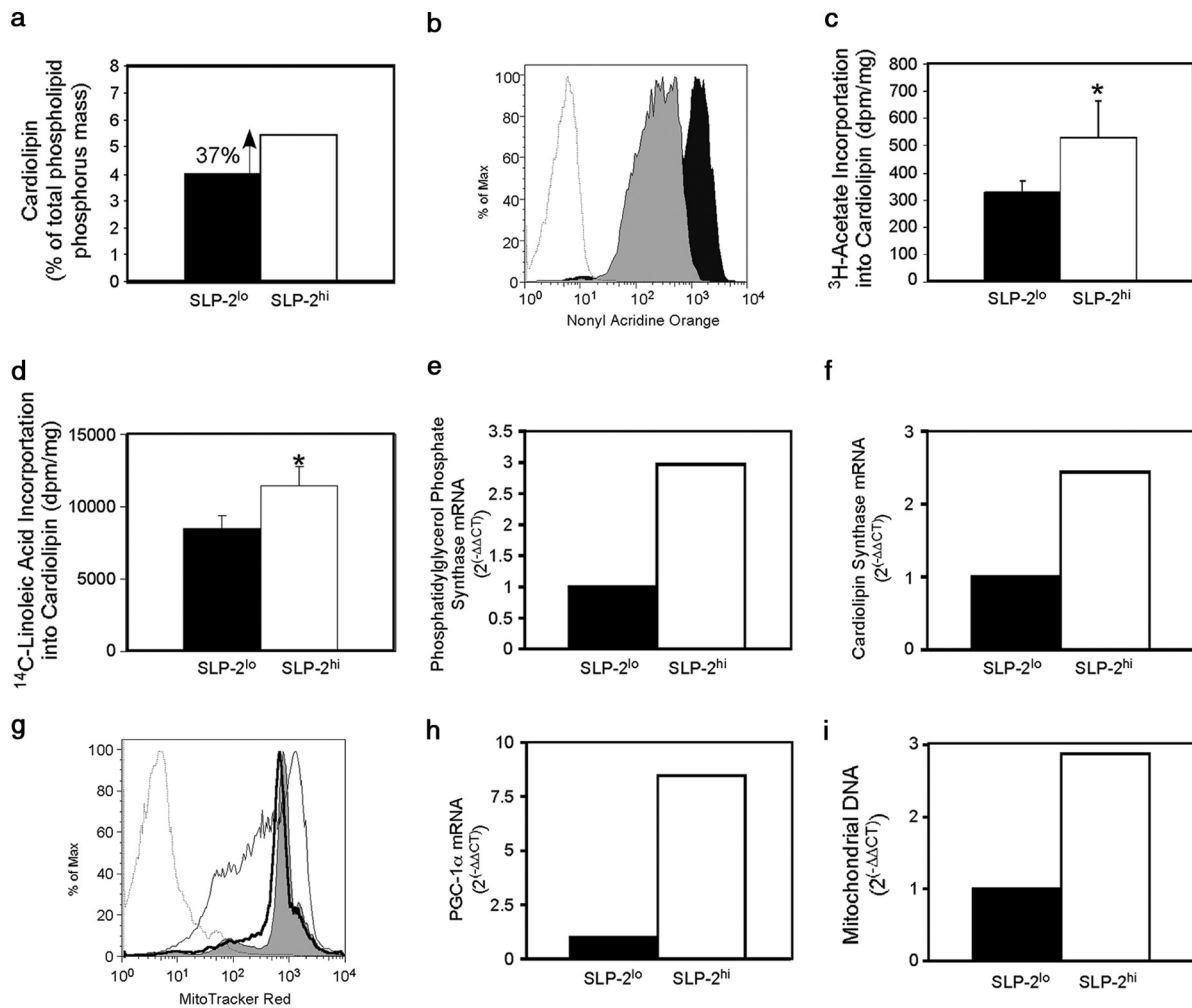


FIG. 3. Induction of SLP-2 expression increases *de novo* cardioliipin biosynthesis, nuclear transcription programs, and mitochondrial DNA replication. (a) Upregulation of SLP-2 expression in Jurkat T cells induces cardioliipin synthesis. Upregulation of SLP-2 expression in T cells (SLP-2^{hi}) was induced with doxycycline and was compared with baseline expression of SLP-2 (SLP-2^{lo}). The pool size of cardioliipin was determined and was expressed as a percentage of the total phospholipid phosphorus mass. (b) Cardioliipin levels in naïve (gray) and *in vitro*-activated (black) PBMCs were measured by flow cytometry after staining with nonyl acridine orange. The result for the unstained control is shown by a dotted line. (c and d) Incorporation of [³H]acetate (c) and [¹⁴C]linoleic acid (d) into cardioliipin in SLP-2^{lo} and SLP-2^{hi} T cells. Data are shown as dpm/mg of total cellular protein. (e and f) Real-time PCR analysis of the transcript levels of phosphatidylglycerol phosphate synthase (e) and cardioliipin synthase (f) in SLP-2^{lo} and SLP-2^{hi} T cells. (g) The mitochondrial mass in naïve (shaded histogram) and *in vitro*-activated PBMC in the absence (thin line) or presence (thick line) of triacsin C was measured by flow cytometry after staining with MitoTracker Red. The result for the unstained control is shown by a dotted line. (h and i) Real-time PCR analysis of the transcript levels of PGC-1 α (h) and of the mitochondrial DNA content (i) in SLP-2^{lo} and SLP-2^{hi} T cells. The results shown here are representative of at least 3 independent experiments. *, $P < 0.05$.

To determine the kinetics of mitochondrial biogenesis in response to SLP-2 upregulation, MitoTracker Red was used to measure mitochondrial mass in PBMCs stimulated with PMA and ionomycin for 48 h. During the first 18 h of stimulation, the cells had a slight decrease in mitochondrial mass, which was recovered by 24 h, and mitochondrial mass was elevated by 48 h of stimulation (Fig. 4a). During this time, SLP-2 and PHB-1 were both found to be upregulated as early as 1 h after stimulation, while PGC-1 α was elevated by 18 h poststimulation (Fig. 4b). This preceded the increase in mitochondrial biogenesis detected by MitoTracker Red at 24 h poststimulation, implying that SLP-2 upregulation in response to T cell activation precedes PGC-1 α upregulation and the subsequent increase in mitochondrial biogenesis.

SLP-2 interacts with prohibitins and binds cardioliipin-enriched microdomains. Next, we examined how upregulation of SLP-2 expression may induce mitochondrial biogenesis. Emerging data suggest that mitochondrial biogenesis is coordinated by a mechanism involving PHB-1 and -2 (17, 35). These proteins localize within phospholipid-enriched, detergent-insoluble microdomains in mitochondrial membranes, and their functional interactome includes genes such as *Ups1* and *Gep1*, which are linked to the synthesis of the mitochondrial membrane phospholipids cardioliipin and phosphatidylethanolamine, respectively (17, 35). We noticed that *Saccharomyces cerevisiae* PHB-2 has a putative transmembrane domain (as predicted by the transmembrane hidden mark or model [TMHMM] algorithm [29]), but neither mouse nor human PHBs have such a domain.

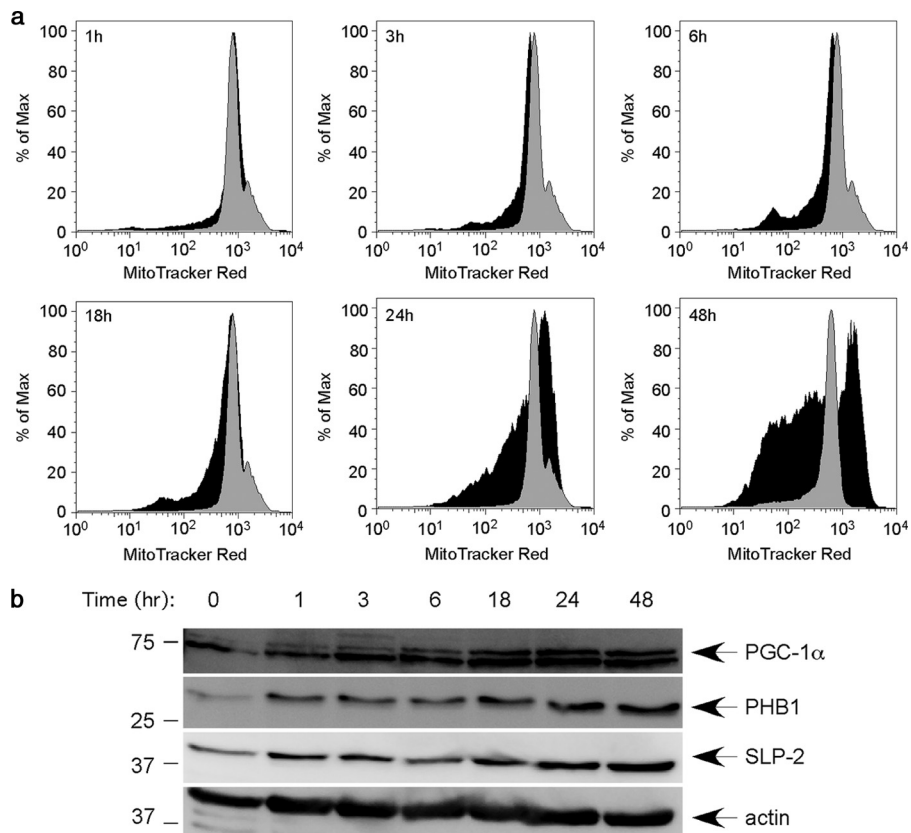


FIG. 4. SLP-2 upregulation precedes PGC-1 α upregulation and mitochondrial biogenesis during T cell activation. (a) PBMCs were stimulated with 1 ng/ml PMA and 100 ng/ml ionomycin for as long as 48 h. At the indicated time points, cells were stained with MitoTracker Red and were analyzed for mitochondrial mass by flow cytometry. Gray, unstimulated cells; black, stimulated cells. (b) Whole-cell lysates were made at each indicated time point during stimulation with PMA and ionomycin. The lysates were separated by SDS-PAGE and were serially blotted for PGC-1 α , PHB-1, SLP-2, and actin.

Of interest, *S. cerevisiae* does not have a homolog of SLP-2, the closest being PHB-1, with a Clustal W score of 15 (41). This suggested that, in mammals, SLP-2 may act to link PHBs and phospholipid-enriched detergent-insoluble microdomains in mitochondrial membranes. Such a possibility is consistent with the observations that PHBs are upregulated in parallel with SLP-2 during activation (38) (Fig. 4b) and that SLP-2 interacts with PHBs (11).

We first confirmed that human SLP-2 interacted with PHB-1 and PHB-2 in T cells by using standard coprecipitation experiments (Fig. 5a). We found that immunoprecipitates of SLP-2 contained both PHB-1 and PHB-2, as previously reported (11). Furthermore, coprecipitation of PHB-1, PHB-2, and SLP-2 increased as the expression of SLP-2 increased with increasing levels of doxycycline in the culture (Fig. 5b). To demonstrate that SLP-2 plays a role in linking prohibitins to phospholipid-enriched detergent-insoluble microdomains, we isolated mitochondria from SLP-2^{lo} and SLP-2^{hi} cells and extracted mitochondrial membranes with Na₂CO₃. We found a higher association of PHB-1 with the mitochondrial membrane fraction in SLP-2^{hi} cells, although the total levels of PHB-1 were similar in the SLP-2^{lo} and SLP-2^{hi} cells (Fig. 5c).

Next, we generated human recombinant SLP-2 (hrSLP-2) and examined the profile of interaction of this protein with different phospholipids by using a phospholipid vesicle co-

precipitation assay (4). In this assay, molecules that interact with phospholipids cosediment with the vesicles, whereas non-interacting proteins remain in the supernatant. We found that hrSLP-2 coprecipitated with cardiolipin vesicles (Fig. 6a, P [pellet fraction]), whereas most of the hrSLP-2 remained in solution when vesicles made of other phospholipids found in mitochondria (phosphatidylcholine and phosphatidylethanolamine) or vesicles made of mostly nonmitochondrial phospholipids (phosphatidylinositol and phosphatidylserine) were used (Fig. 6a, S [supernatant fraction]). Of interest, hrSLP-2 bound to phosphatidylglycerol vesicles in smaller amounts, a finding likely due to the fact that cardiolipin is a composite of two phosphatidylglycerol molecules. To further investigate the association of hrSLP-2 with cardiolipin, we prepared phospholipid vesicles containing cardiolipin along with the other two major phospholipids in mitochondria, phosphatidylcholine and phosphatidylethanolamine, at ratios of 1:1:1 (33% CL, 33% PC, 33% PE), 2.5:0.25:0.25 (83% CL, 8% PC, 8% PE), and 2.75:0.12:0.12 (92% CL, 4% PC, 4% PE). The interaction between hrSLP-2 and cardiolipin was selective and titrated with the enrichment of this phospholipid in vesicles also containing phosphatidylcholine and phosphatidylethanolamine (Fig. 6b). These data demonstrate that SLP-2 binds to the prohibitin complex as well as to cardiolipin-enriched membrane microdo-

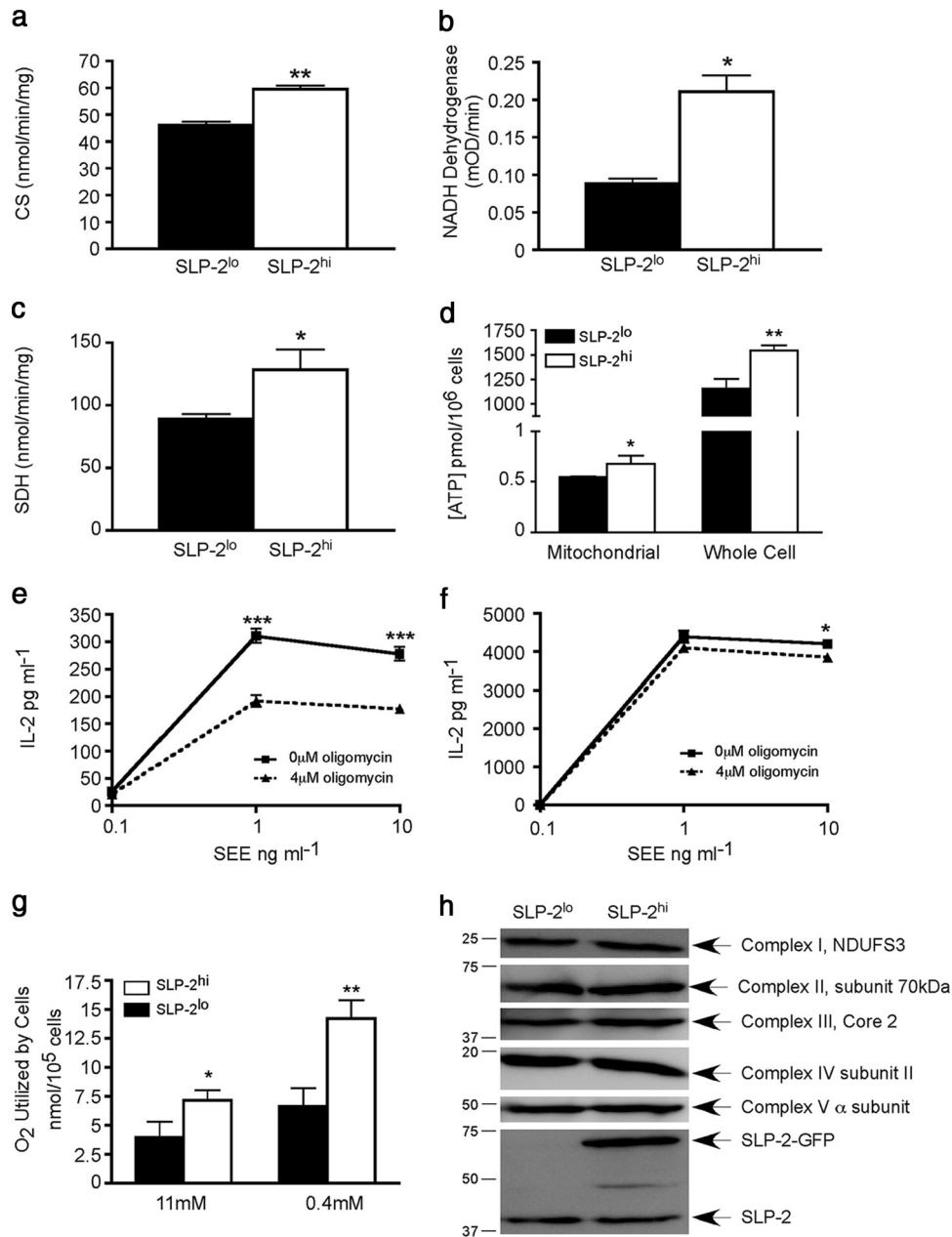


FIG. 7. Induction of SLP-2 expression is associated with higher mitochondrial activity. (a) Citrate synthase (CS) activity was measured in SLP-2^{lo} and SLP-2^{hi} Jurkat T cells. Data are means and standard deviations for triplicate samples; **, $P < 0.01$. Data are expressed as nmol/min/mg mitochondrial protein. (b) NADH dehydrogenase was measured in SLP-2^{lo} and SLP-2^{hi} Jurkat T cells, plotted as in panel a. *, $P < 0.05$. (c) Succinate dehydrogenase (SDH) was measured in SLP-2^{lo} and SLP-2^{hi} Jurkat T cells, plotted as in panel a. *, $P < 0.05$. Data are expressed as nmol/min/mg mitochondrial protein. (d) Mitochondrial and total cellular ATP levels were measured in SLP-2^{lo} and SLP-2^{hi} Jurkat T cells. Means and standard deviations for triplicate samples are plotted. *, $P < 0.05$; **, $P < 0.01$. (e and f) IL-2 levels in culture supernatants of SLP-2^{lo} (e) and SLP-2^{hi} (f) Jurkat T cells pretreated or not with oligomycin (4 μM) and stimulated with antigen-presenting cells and SEE for 24 h. Means and standard deviations for triplicate samples are plotted. Asterisks indicate significant differences (*, $P < 0.05$; ***, $P < 0.001$) as determined by analysis of variance (ANOVA) with a Bonferroni posttest. (g) Oxygen consumption was measured in SLP-2^{lo} and SLP-2^{hi} T cells in media containing high (11 mM) or low (0.4 mM) glucose levels. Means and standard deviations for triplicate samples are plotted. Asterisks indicate significant differences (*, $P < 0.05$; **, $P < 0.01$) as determined by ANOVA with a Bonferroni posttest. (h) Mitochondria were isolated from SLP-2^{lo} and SLP-2^{hi} cells, separated by SDS-PAGE, and serially blotted for subunits of each complex of the respiratory chain as well as SLP-2.

increase in ATP levels in SLP-2^{hi} T cells correlated with increased resistance to depletion of mitochondrial ATP with oligomycin, as evidenced by increased T-cell responses, indicated by increased IL-2 production. In these experiments,

oligomycin-treated SLP-2^{lo} T cells and SLP-2^{hi} T cells were stimulated with antigen-presenting cells and the superantigen staphylococcal enterotoxin E (SEE), and the production of interleukin-2 (IL-2) was determined after 24 h of stimulation.

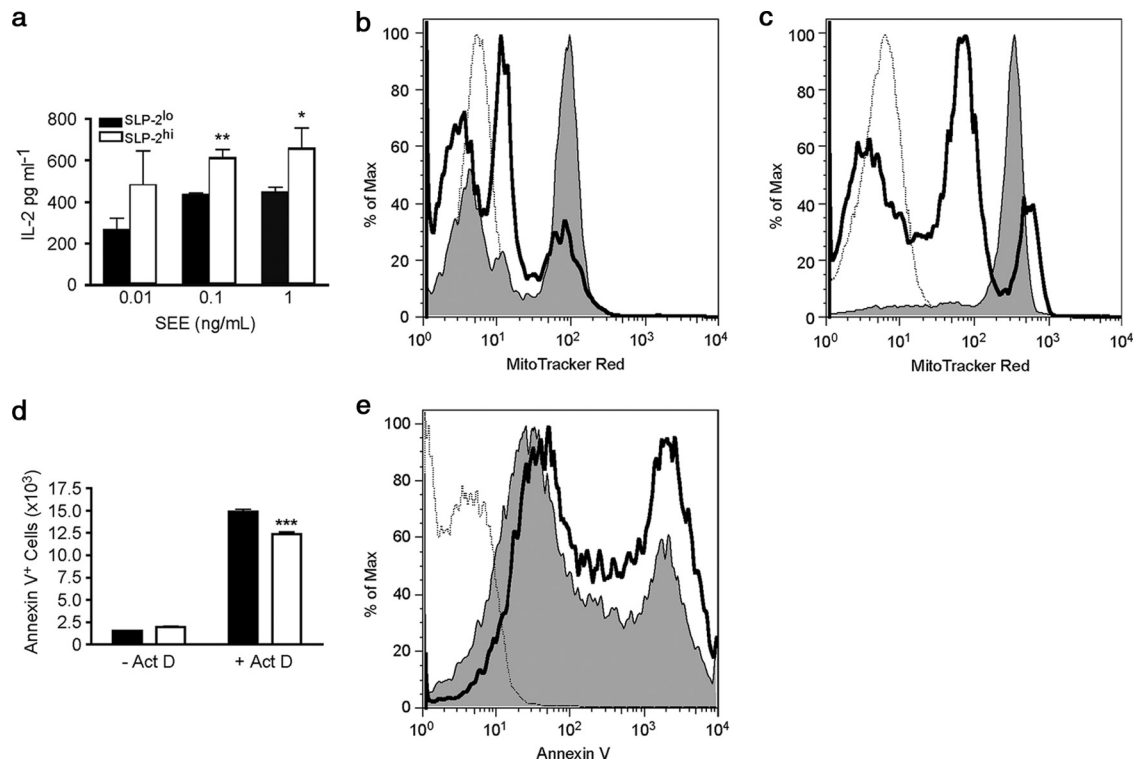


FIG. 8. SLP-2 upregulation increases T cell responses and protects against apoptosis. (a) Human peripheral blood T cells nucleofected with doxycycline-inducible SLP-2-GFP and expressing high levels of SLP-2 (SLP-2^{hi}) upon doxycycline induction produce significantly more IL-2 in response to stimulation with antigen-presenting cells and SEE than control (noninduced) SLP-2-GFP-transfected T cells. **, $P < 0.01$; *, $P < 0.05$. (b) SLP-2^{hi} primary T cells are less susceptible to actinomycin D-induced apoptosis. Human PBMCs were transiently transfected with doxycycline-inducible SLP-2-GFP and were cultured with (SLP-2^{hi}) (shaded histogram) or without (SLP-2^{lo}) (open histogram) doxycycline and with actinomycin D (5 μ g/ml) for 3 h at 37°C. Cell death was measured by MitoTracker Red staining, which was analyzed by flow cytometry. (c) Upregulation of SLP-2 expression in doxycycline-inducible SLP-2-GFP-transfected Jurkat T cells results in increased resistance to actinomycin D-induced apoptosis. SLP-2^{hi} (shaded histogram) and SLP-2^{lo} (open histogram) T cells were treated with 5 μ g/ml actinomycin D for 3 h at 37°C. (d) SLP-2^{hi} (open bars) and SLP-2^{lo} (filled bars) T cells were treated with actinomycin D (Act D) and were stained for annexin V, an alternative marker of apoptosis. ***, $P < 0.001$. (e) One representative flow cytometry plot of annexin V staining of SLP-2^{hi} (shaded histogram) and SLP-2^{lo} (open histogram) cells after induction of apoptosis with actinomycin D. The result for the unstained control is shown by a dotted line. The data are representative of three independent experiments.

Oligomycin treatment significantly reduced the IL-2 response of SLP-2^{lo} T cells to SEE ($P < 0.001$) (Fig. 7e) but did not affect the response of SLP-2^{hi} T cells (Fig. 7f). Consistent with our previous findings, SLP-2^{hi} T cells had a higher IL-2 response than SLP-2^{lo} T cells (28).

Given that the generation of ATP by OXPHOS is linked to the respiratory chain in the mitochondrial inner membrane, we examined the effect of modulating SLP-2 expression on oxygen consumption by T cells. We found that SLP-2^{hi} T cells had slightly but significantly higher oxygen consumption than SLP-2^{lo} T cells ($P < 0.05$). In a low-glucose medium, SLP-2^{hi} T cells had much higher oxygen consumption than SLP-2^{lo} T cells ($P < 0.01$) (Fig. 7g). This is expected, since cells rely more heavily on OXPHOS under low-glucose conditions. Therefore, we concluded that upregulation of SLP-2 expression is associated with increased oxygen consumption and OXPHOS, leading to increased ATP stores in the cell.

Cardiolipin plays an essential role in the mitochondrial protein import machinery (26), and as such, the increase in cardiolipin levels seen in response to SLP-2 upregulation could lead to an increased rate of protein transport into the mitochondria. If so, the increased enzymatic rates we detected

in SLP-2^{hi} cells could be due to elevated protein levels in the mitochondria. To test this, mitochondria were isolated from SLP-2^{lo} and SLP-2^{hi} cells, and lysates from these mitochondria were blotted for representative subunits of each complex of the respiratory chain. SLP-2^{lo} and SLP-2^{hi} cells had similar protein levels for each complex of the respiratory chain (Fig. 7h), indicating that the increase in enzymatic activity seen in the SLP-2-overexpressing cells was not due to increased levels or increased translocation of electron transport complexes into mitochondria.

Upregulation of SLP-2 expression increases T cell responses and resistance to apoptosis. In light of the significantly enhanced mitochondrial biogenesis and function associated with SLP-2 upregulation, we examined the physiological effects of these changes by looking at the functional response of primary human T cells in which SLP-2 expression was upregulated. As shown in Fig. 8a, peripheral blood T cells from normal volunteers transiently nucleofected with doxycycline-inducible SLP-2-GFP cDNA and expressing high levels of SLP-2 produced significantly higher levels of IL-2 ($P < 0.05$) upon stimulation with SEE and antigen-presenting cells. In addition, these cells showed increased resistance to apoptosis through the intrinsic

pathway (Fig. 8b). Such resistance to apoptosis was also observed in response to actinomycin D in Jurkat SLP-2^{hi} T cells (Fig. 8c). As an additional marker of apoptosis, actinomycin D-induced cell death was also measured by an increase in annexin V labeling. In agreement with the loss of transmembrane potential as measured by MitoTracker Red, SLP-2^{hi} cells also showed lower annexin V staining, which is indicative of protection against the induction of the intrinsic apoptosis pathway (Fig. 8d and e). Thus, consistent with the increased mitochondrial biogenesis and function, upregulation of SLP-2 expression enhances cell function.

DISCUSSION

The function of stomatins and other proteins sharing the stomatin/prohibitin/flotillin/HflK (SPFH) domain remain enigmatic. It has been proposed that through this domain, stomatins, PHBs, and flotillins interact with different cell membranes and facilitate signaling. We report here that SLP-2, a mitochondrial member of the stomatin family, binds cardiolipin and may help to recruit PHBs to cardiolipin-enriched microdomains. Furthermore, upregulation of SLP-2 expression is associated with increased mitochondrial biogenesis and function, ultimately resulting in enhanced effector cell function.

Our data show that SLP-2 binds cardiolipin-enriched microdomains in a way that titrates with the content of cardiolipin in phospholipid membranes. The mitochondrial membrane is composed of 40% phosphatidylcholine, 30% phosphatidylethanolamine, and 10 to 15% phosphatidylinositol and cardiolipin (36). But the cardiolipin content in the mitochondrial membrane is not homogeneously distributed. Our data suggest that SLP-2 can bind to clusters of cardiolipin, i.e., microdomains with a much higher localized cardiolipin concentration. This selective binding of SLP-2 to cardiolipin is reminiscent of the observation that two other members of the stomatin/PHB/flotillin/HflK superfamily (MEC-2 and podocin) bind cholesterol (24) and leads us to propose that SPFH domain-containing proteins bind to selective phospholipid-enriched membrane microdomains and may act as markers that recruit other proteins to the lipid microdomains. How these proteins bind lipids is still unknown. The binding of SLP-2 to cardiolipin in the mitochondrial inner membrane is likely independent of transmembrane insertion, since SLP-2 lacks a putative transmembrane domain (43).

Upregulation of SLP-2 expression increases cardiolipin synthesis and mitochondrial biogenesis. Recent evidence indicates that these two processes are tightly coordinated (17), likely through the PHB functional interactome, which includes genes involved in phospholipid synthesis, such as *Upl1*, whose deletion, in yeast, translates into a marked decrease in cardiolipin content (35). Although we have not shown a direct interaction among PHBs, SLP-2, and cardiolipin, our data suggest that SLP-2 may bring PHBs to cardiolipin and may contribute to the organization of cardiolipin-enriched microdomains in the mitochondrial inner membrane (3). Data from our laboratory using T cell-specific SLP-2 knockout mice seem to corroborate this model (D. A. Christie et al., unpublished data). This possible mechanism accommodates the upregulation of both SLP-2 and PHBs during T cell activation (38) and the detection of both proteins in detergent-insoluble microdomains of

cell membranes (i.e., cardiolipin-enriched microdomains in the mitochondrial inner membrane and cholesterol-enriched microdomains in the plasma membrane) (13, 27, 28, 33). In this context, an increase in SLP-2 levels as a result of cell activation would increase the interaction of PHBs with cardiolipin in the mitochondrial inner membrane and activate the PHB functional interactome, leading to *de novo* cardiolipin synthesis.

Using human T cell activation as a model, we have shown that upregulation of SLP-2 expression is a molecular step between mitochondrial biogenesis and cell activation and function. SLP-2 does not seem to be critical under resting conditions, as suggested by the absence or very low level of SLP-2 expression in resting naïve T cells. However, during T cell activation, SLP-2 expression is dramatically upregulated, and this increases T cell function, leading to increased IL-2 production and increased resistance to apoptosis through the intrinsic pathway. PHBs are also upregulated during T cell activation (38), whereas PHB-2 deletion decreases the ability of cells to proliferate and increases their sensitivity to apoptosis through the intrinsic pathway (32). These observations corroborate the model proposed here by which SLP-2–PHB complexes would act in concert to regulate mitochondrial biogenesis and function during T cell activation. Of interest, modulation of PHB-2 levels also alters OPA-1 levels (e.g., cells lacking PHB-2 have impaired processing of OPA-1 [3]), and in our experiments, T cells overexpressing SLP-2 have increased OPA-1 levels.

The increased mitochondrial function observed in SLP-2-overexpressing cells is in line with the observation that SLP-2 controls the stability and the assembly of electron transport complexes (1, 23). This is further corroborated by emerging data from our laboratory using T cell-specific SLP-2-deficient mice, showing that a lack of SLP-2 is associated with decreased recruitment of PHB-1 to cardiolipin-enriched mitochondrial membranes, as well as a loss of complex I subunits (D. A. Christie et al., unpublished data). Optimal assembly of these complexes may require the formation of specialized membrane microdomains, and this would correlate with increased respiratory chain function. Of interest, SLP-2 is required for mitochondrial hyperfusion (42), a phenomenon linked with increased metabolic demands and cellular stress. Levels of both OPA-1 and mitofusin-2, proteins required for this process, were increased upon SLP-2 upregulation, but cytochrome *c* levels were not. It is possible that SLP-2 expression specifically increases the expression of proteins involved in mitochondrial fusion, or prevents these proteins from degradation, without altering the expression of other mitochondrial proteins.

Taken together, the evidence presented here leads us to propose that the binding of SLP-2 to cardiolipin recruits PHBs, helping to form cardiolipin-enriched membrane microdomains in which the respiratory chain components are optimally assembled. The formation of these microdomains is likely the result of the self-oligomerizing properties of SLP-2 (43). The increase in respiratory chain function may then induce further cardiolipin synthesis through its effect on the pH gradient across the mitochondrial inner membrane (18), enhancing mitochondrial biogenesis. The result of this proposed mechanism is the provision of the enhanced mitochondrial function required for an optimal T cell response.

How the increased mitochondrial membrane formation

increases nuclear transcription and mitochondrial DNA replication, both required to increase mitochondrial numbers, remains to be determined. A retrograde nuclear signaling pathway in yeast is starting to emerge, but little is known about this pathway in mammalian cells. Specific signals may involve mitochondrial stress, since it has been shown that mitochondrial dysfunction increases nuclear transcription (40). In this context, SLP-2 may play a role by regulating mitochondrial membrane biogenesis and its subsequent effect of calcium-dependent signaling, which has been linked to the activation of retrograde signaling (6).

In summary, we have shown that increased levels of SLP-2, seen, for example, during lymphocyte activation, stimulate mitochondrial biogenesis and function, providing for the energetic requirements of activation. Such a function involves the binding of SLP-2 and its interacting partners (PHBs) to cardiolipin to form membrane microdomains in which respiratory complexes are optimally assembled. The ultimate result of this function is the net enhancement of effector cell functions.

ACKNOWLEDGMENTS

We thank Heidi McBride, Jean-Claude Martinou, Fred Possmayer, and the members of the Madrenas laboratory for helpful discussions in the course of this work.

This research was supported by the Canadian Institutes of Health Research. D.A.C. holds a CIHR Doctoral Studentship. G.M.H. holds a Canada Research Chair in Molecular Cardiolipin Metabolism, and J.M. holds a Canada Research Chair in Immunobiology.

REFERENCES

- Acin-Perez, R., P. Fernandez-Silva, M. L. Peleato, A. Perez-Martos, and J. A. Enriquez. 2008. Respiratory active mitochondrial supercomplexes. *Mol. Cell* **32**:529–539.
- Arp, J., et al. 2003. Regulation of T-cell activation by phosphodiesterase 4B2 requires its dynamic redistribution during immunological synapse formation. *Mol. Cell. Biol.* **23**:8042–8057.
- Artal-Sanz, M., and N. Tavernarakis. 2009. Prohibitin and mitochondrial biology. *Trends Endocrinol. Metab.* **20**:394–401.
- Bakolitsa, C., J. M. de Pereda, C. R. Bagshaw, D. R. Critchley, and R. C. Liddington. 1999. Crystal structure of the vinculin tail suggests a pathway for activation. *Cell* **99**:603–613.
- Baroja, M. L., et al. 2000. The inhibitory function of CTLA-4 does not require its tyrosine phosphorylation. *J. Immunol.* **164**:49–55.
- Biswas, G., et al. 1999. Retrograde Ca^{2+} signaling in C2C12 skeletal myocytes in response to mitochondrial genetic and metabolic stress: a novel mode of inter-organelle crosstalk. *EMBO J.* **18**:522–533.
- Bueno, C., et al. 2006. Bacterial superantigens bypass Lck-dependent T cell receptor signaling by activating a $G\alpha 11$ -dependent, PLC- β -mediated pathway. *Immunity* **25**:67–78.
- Carpentieri, U., and L. A. Sordahl. 1980. Respiratory and calcium transport functions of mitochondria isolated from normal and transformed human lymphocytes. *Cancer Res.* **40**:221–224.
- Chau, T. A., et al. 2009. Toll-like receptor 2 ligands on the staphylococcal cell wall downregulate superantigen-induced T cell activation and prevent toxic shock syndrome. *Nat. Med.* **15**:641–648.
- Cote, H. C., et al. 2002. Changes in mitochondrial DNA as a marker of nucleoside toxicity in HIV-infected patients. *N. Engl. J. Med.* **346**:811–820.
- Da Cruz, S., et al. 2008. SLP-2 interacts with prohibitins in the mitochondrial inner membrane and contributes to their stability. *Biochim. Biophys. Acta* **1783**:904–911.
- D'Souza, A. D., N. Parikh, S. M. Kaech, and G. S. Shadel. 2007. Convergence of multiple signaling pathways is required to coordinately up-regulate mtDNA and mitochondrial biogenesis during T cell activation. *Mitochondrion* **7**:374–385.
- Foster, L. J., C. L. De Hoog, and M. Mann. 2003. Unbiased quantitative proteomics of lipid rafts reveals high specificity for signaling factors. *Proc. Natl. Acad. Sci. U. S. A.* **100**:5813–5818.
- Fox, C. J., P. S. Hammerman, and C. B. Thompson. 2005. Fuel feeds function: energy metabolism and the T-cell response. *Nat. Rev. Immunol.* **5**:844–852.
- Frauwirth, K. A., et al. 2002. The CD28 signaling pathway regulates glucose metabolism. *Immunity* **16**:769–777.
- Frauwirth, K. A., and C. B. Thompson. 2004. Regulation of T lymphocyte metabolism. *J. Immunol.* **172**:4661–4665.
- Gohil, V. M., and M. L. Greenberg. 2009. Mitochondrial membrane biogenesis: phospholipids and proteins go hand in hand. *J. Cell Biol.* **184**:469–472.
- Gohil, V. M., et al. 2004. Cardiolipin biosynthesis and mitochondrial respiratory chain function are interdependent. *J. Biol. Chem.* **279**:42612–42618.
- Green, J. B., and J. P. Young. 2008. Slp1ins: ancient origin, duplication and diversification of the stomatin protein family. *BMC Evol. Biol.* **8**:44.
- Hajek, P., A. Chomyn, and G. Attardi. 2007. Identification of a novel mitochondrial complex containing mitofusin 2 and stomatin-like protein 2. *J. Biol. Chem.* **282**:5670–5681.
- Hatch, G. M., and G. McClarty. 1996. Regulation of cardiolipin biosynthesis in H9c2 cardiac myoblasts by CTP. *J. Biol. Chem.* **271**:25810–25816.
- Haufl, K., D. Linda, and G. M. Hatch. 2009. Mechanism of the elevation in cardiolipin during HeLa cell entry into the S-phase of the human cell cycle. *Biochem. J.* **417**:573–582.
- Houtkooper, R. H., and F. M. Vaz. 2008. Cardiolipin, the heart of mitochondrial metabolism. *Cell. Mol. Life Sci.* **65**:2493–2506.
- Huber, T. B., et al. 2006. Podocin and MEC-2 bind cholesterol to regulate the activity of associated ion channels. *Proc. Natl. Acad. Sci. U. S. A.* **103**:17079–17086.
- Jacobson, J., M. R. Duchon, and S. J. Heales. 2002. Intracellular distribution of the fluorescent dye nonyl acridine orange responds to the mitochondrial membrane potential: implications for assays of cardiolipin and mitochondrial mass. *J. Neurochem.* **82**:224–233.
- Joshi, A. S., J. Zhou, V. M. Gohil, S. Chen, and M. L. Greenberg. 2009. Cellular functions of cardiolipin in yeast. *Biochim. Biophys. Acta* **1793**:212–218.
- Kim, K. B., et al. 2006. Oxidation-reduction respiratory chains and ATP synthase complex are localized in detergent-resistant lipid rafts. *Proteomics* **6**:2444–2453.
- Kirchhof, M. G., et al. 2008. Modulation of T cell activation by stomatin-like protein 2. *J. Immunol.* **181**:1927–1936.
- Krogh, A., B. Larsson, G. von Heijne, and E. L. Sonnhammer. 2001. Predicting transmembrane protein topology with a hidden Markov model: application to complete genomes. *J. Mol. Biol.* **305**:567–580.
- Livak, K. J., and T. D. Schmittgen. 2001. Analysis of relative gene expression data using real-time quantitative PCR and the $2^{-\Delta\Delta CT}$ method. *Methods* **25**:402–408.
- Lowry, O. H., N. J. Rosebrough, A. L. Farr, and R. J. Randall. 1951. Protein measurement with the Folin phenol reagent. *J. Biol. Chem.* **193**:265–275.
- Merkwirth, C., et al. 2008. Prohibitins control cell proliferation and apoptosis by regulating OPA1-dependent cristae morphogenesis in mitochondria. *Genes Dev.* **22**:476–488.
- Mielenz, D., et al. 2005. Lipid rafts associate with intracellular B cell receptors and exhibit a B cell stage-specific protein composition. *J. Immunol.* **174**:3508–3517.
- Nagy, G., M. Barcza, N. Gonchoroff, P. E. Phillips, and A. Perl. 2004. Nitric oxide-dependent mitochondrial biogenesis generates Ca^{2+} signaling profile of lupus T cells. *J. Immunol.* **173**:3676–3683.
- Osman, C., et al. 2009. The genetic interactome of prohibitins: coordinated control of cardiolipin and phosphatidylethanolamine by conserved regulators in mitochondria. *J. Cell Biol.* **184**:583–596.
- Osman, C., D. R. Voelker, and T. Langer. 2011. Making heads or tails of phospholipids in mitochondria. *J. Cell Biol.* **192**:7–16.
- Owczarek, C. M., et al. 2001. A novel member of the STOMATIN/EPB72/mec-2 family, stomatin-like 2 (STOML2), is ubiquitously expressed and localizes to HSA chromosome 9p13.1. *Cytogenet. Cell Genet.* **92**:196–203.
- Ross, J. A., Z. S. Nagy, and R. A. Kirken. 2008. The PHB1/2 phosphocomplex is required for mitochondrial homeostasis and survival of human T cells. *J. Biol. Chem.* **283**:4699–4713.
- Rouser, G., S. Fleischer, and A. Yamamoto. 1970. Two dimensional thin layer chromatographic separation of polar lipids and determination of phospholipids by phosphorus analysis of spots. *Lipids* **5**:494–496.
- Scarpulla, R. C. 2008. Transcriptional paradigms in mammalian mitochondrial biogenesis and function. *Physiol. Rev.* **88**:611–638.
- Thompson, J. D., D. G. Higgins, and T. J. Gibson. 1994. CLUSTAL W: improving the sensitivity of progressive multiple sequence alignment through sequence weighting, position-specific gap penalties and weight matrix choice. *Nucleic Acids Res.* **22**:4673–4680.
- Tondera, D., et al. 2009. SLP-2 is required for stress-induced mitochondrial hyperfusion. *EMBO J.* **28**:1589–1600.
- Wang, Y., and J. S. Morrow. 2000. Identification and characterization of human SLP-2, a novel homologue of stomatin (band 7.2b) present in erythrocytes and other tissues. *J. Biol. Chem.* **275**:8062–8071.